Am J Transl Res 2026;18(5):3972-3987
www.ajtr.org /ISSN:1943-8141/AJTR0170413

Original Article

LncRNA EWSAT1 promotes colorectal cancer progression by regulating the miR-330-5p/CPEB4 axis

Chu-Xian Tang[1], Dong-Fang Xie[2], Xin-Bin Wang[2], Hai-Ming Yu[3], Fang-Zhou Xing[2], Zu-Hao Zhao[2], Tao Yang[2]

[1]Qingdao Medical College of Qingdao University, Qingdao 266073, Shandong, China; [2]Department of General Surgery, Qingdao Central Hospital, University of Health and Rehabilitation Sciences, Qingdao 266042, Shandong, China; [3]Department of Oncology, Shandong Provincial Key Medical and Health Discipline, Qingdao Central Hospital, University of Health and Rehabilitation Sciences, Qingdao 266042, Shandong, China

Received November 30, 2025; Accepted May 13, 2026; Epub May 15, 2026; Published May 30, 2026

Abstract: Ewing sarcoma-associated transcript 1 (EWSAT1) has been implicated in colorectal cancer (CRC) progression, but its downstream regulatory mechanisms remain unclear. This study aimed to investigate whether EWSAT1 promotes the malignant progression of CRC via the miR-330-5p/CPEB4 axis. The expression levels of EWSAT1, miR-330-5p, and CPEB4 in 30 pairs of CRC tissues and adjacent normal tissues were detected by qRT-PCR. The effects of siRNA-mediated EWSAT1 knockdown on cell proliferation, migration, invasion, and apoptosis were evaluated in HCT-15 and HCT-116 cells. RNA pull-down and dual-luciferase reporter assays were performed to verify the interactions between EWSAT1 and miR-330-5p, as well as between miR-330-5p and the 3'-UTR of CPEB4. Additionally, qRT-PCR, Western blot analysis, and rescue assays (via miR-330-5p inhibition or CPEB4 overexpression) were employed to clarify the functional role of this regulatory axis. The expression levels of EWSAT1 and CPEB4 were increased, while that of miR-330-5p was decreased in CRC tissues compared with adjacent normal tissues. Knockdown of EWSAT1 significantly inhibited the proliferation, migration, and invasion of CRC cells, and promoted their apoptosis. Mechanistically, EWSAT1 could directly bind to miR-330-5p, thereby alleviating the inhibitory effect of miR-330-5p on CPEB4. Inhibition of miR-330-5p or overexpression of CPEB4 could partially reverse the suppression of malignant phenotypes induced by EWSAT1 knockdown. Furthermore, high CPEB4 expression was associated with poorer survival outcomes in CRC patients. In conclusion, EWSAT1 promotes the malignant phenotypes of CRC cells by regulating the miR-330-5p/CPEB4 axis. This molecular axis may provide new insights into the mechanisms of CRC progression and potential targeted interventions.

Keywords: Colorectal cancer, Ewing sarcoma associated transcript 1, miR-330-5p, cytoplasmic polyadenylation element binding protein 4

Introduction

Worldwide, colorectal cancer (CRC) is the 3rd most diagnosed cancer and the 2nd leading cause of cancer-related death [1]. In the U.S., improved therapeutic strategies have increased the 5-year survival rate of CRC patients to 65%, largely due to advances in surgical techniques [2]. In China, the 5-year survival rate of CRC patients is as high as 56.9%, and it is on the rise with the improvement of medical standards [3]. However, due to insufficient awareness of red-flag symptoms (e.g., persistent diarrhea, hematochezia), most CRC cases are not diagnosed at an early stage. This delay in diagnosis leads to delayed treatment, which can exacerbate disease progression and reduce the 5-year survival rate [4, 5]. Therefore, elucidating the core molecular mechanisms underlying CRC initiation and metastasis, as well as identifying novel diagnostic biomarkers, is a crucial research priority.

Long non-coding RNAs (lncRNAs), defined as transcripts longer than 200 nucleotides that lack functional open reading frames, play crucial roles in various biological processes, including transcriptional regulation, epigenetic marks, molecular stability, translation, and post-translational modifications [6]. Accumulating evidence has established lncRNAs as pivotal regulators in cancer, influencing not only canonical

https://doi.org/10.62347/JXWL4393

malignant behaviors like proliferation and invasion but also metabolic reprogramming [7]. LncRNAs act as microRNA (miRNA) sponges via a competitive endogenous RNA (ceRNA) mechanism, thereby modulating downstream gene expression [8]. Multiple lncRNAs, including ITGB8-AS1, SNHG16, and MIR600HG, act as critical regulators of CRC progression by modulating tumor growth, migration, and invasion [9-11]. Ewing sarcoma-associated transcript 1 (EWSAT1), a member of lncRNAs, was first identified in Ewing's sarcoma and can promote cell proliferation and metastasis in Ewing sarcoma cell lines [12]. A previous mechanistic study demonstrated that EWSAT1 upregulation orchestrates multiple oncogenic processes in CRC, including enhanced proliferative capacity, invasive potential, and epithelial-mesenchymal transition dynamics [13]. However, the molecular mechanisms by which EWSAT1 regulates CRC progression remain poorly defined.

MicroRNAs (miRNAs) are a family of naturally occurring, evolutionarily conserved small noncoding RNA molecules, typically ~22 nucleotides in length. They bind to complementary sequences in the 3'-untranslated regions (3'-UTRs) of their target messenger RNAs (mRNAs), thereby suppressing gene expression [14]. This regulatory capacity allows them to influence a broad range of cellular activities, including developmental processes [15]. Accumulating evidence has identified miR-330-5p as a crucial player in various malignancies, including breast cancer [16], bladder cancer [17], cervical cancer [18], and CRC [19]. However, the exact role of miR-330-5p in CRC pathogenesis remains to be fully elucidated.

Vertebrates express four well-characterized members of the Cytoplasmic Polyadenylation Element Binding Protein (CPEB) family: CPEB1, CPEB2, CPEB3, and CPEB4 [20]. Despite functional diversity among these members, the CPEB family plays a critical role in regulating tumor pathogenesis and angiogenesis [21]. However, the regulatory mechanisms of CPEB family members in CRC remain incompletely understood. Thus, this study aimed to clarify the exact molecular mechanisms by which CPEB family members affect CRC progression.

This study revealed the oncogenic function of EWSAT1 in CRC by regulating the miR-330-5p/CPEB4 axis. Our findings reveal a previously unreported pathway in CRC and highlight the translational potential of EWSAT1 as both a diagnostic biomarker and a therapeutic candidate.

Materials and methods

Patients and tissue sample

Thirty patients who underwent laparoscopic radical resection for CRC at the Department of Abdominal Tumor Surgery, Qingdao Central Hospital of Rehabilitation University between May 2021 and May 2024 were enrolled in this study. Surgically removed tumor tissues and matched adjacent normal tissues were collected, immediately cryopreserved in liquid nitrogen after resection, and stored at -80°C. The study protocol was approved by the Ethics Committee of Qingdao Central Hospital of Rehabilitation University. Written informed consent was obtained from all participants.

Inclusion criteria were as follows: (1) histopathologically confirmed primary colorectal adenocarcinoma; (2) successful radical surgical resection with intact tumor tissue and paired adjacent normal tissue obtained; (3) no preoperative anticancer treatment, including chemotherapy, radiotherapy, immunotherapy, or targeted therapy; (4) complete clinical and pathological data; (5) sufficient tissue quantity and quality for subsequent experimental analysis.

Exclusion criteria were as follows: (1) recurrent CRC or metastatic colorectal tumors originating from other primary tumors; (2) prior antitumor treatment; (3) concurrent malignant tumors or severe systemic diseases; (4) insufficient or poor-quality tissue samples that did not meet study requirements. Adjacent normal tissue was defined as histopathologically confirmed non-cancerous tissue located at least 5 cm from the tumor margin, with no evidence of tumor cell infiltration. Expression levels of EWSAT1, miR-330-5p, and CPEB4 in CRC and adjacent normal tissues were assessed by qRT-PCR using surgically collected samples.

Cell culture

Human CRC cell lines HCT-15 (Cat# CX 0198), HCT-116 (Cat# CX 0064), and the human embryonic kidney cell line HEK293T (Cat# CX 0001) were purchased from Boster Biological

Table 1. Transfection sequence

Gene	Sequences (5'-3')
Si-EWSAT1	Sense (S): CUAUUUCUUCCUGCAACAUTT
	Antisense (AS): AUGUUGCAGGAAGAAAUAGAG
miR-330-5p mimics	S: UCUCUGGGCCUGUGUCUUAGGC
	AS: CUAAGACACAGGCCCAGAGAUU
miR-330-5p antagomir	S: GCCUAAGACACAGGCCCAGAGA
MicroRNA inhibitor N.C.	CAGUACUUUUGUGUAGUACAA
Negative control	S: UUCUCCGAACGUGUCACGUTT
	AS: ACGUGACACGUUCGGAGAATT

Technology (Wuhan, China). All cell lines were authenticated by the supplier, and their identities were verified by short tandem repeat profiling. Mycoplasma testing was performed after cell thawing, and all results were negative. Only cells at low passage numbers were used in subsequent experiments. HCT-15 cells were cultured in RPMI-1640 medium, HCT-116 cells were cultured in McCoy's 5A medium, and HEK293T cells were cultured in DMEM medium. All culture media were purchased from Meilunbio (Liaoning, China) and supplemented with 10% fetal bovine serum and 1% penicillin-streptomycin. All cells were maintained in a humidified incubator at 37°C with 5% CO_2.

Cell transfection

For functional studies, HCT-15 and HCT-116 cells were subjected to EWSAT1 knockdown, miR-330-5p overexpression, miR-330-5p inhibition, or CPEB4 overexpression. The small interfering RNA targeting EWSAT1 (si-EWSAT1), siRNA negative control, miR-330-5p mimics, mimic negative control, miR-330-5p antagomir, and antagomir negative control were synthesized by GenePharma (Jiangsu, China). The CPEB4 overexpression plasmid and its corresponding empty vector control were also constructed by GenePharma. Sequence information for all oligonucleotides and plasmids is provided in **Table 1**.

Before transfection, cells were seeded in 6-well plates and cultured until they reached 60-70% confluence. The final concentration of si-EWSAT1, miR-330-5p mimics, and their respective negative controls was 50 nM, whereas the final concentration of miR-330-5p antagomir and its negative control was 100 nM. Each CPEB4 overexpression plasmid or empty vector control was used at 2 μg per well. Transfections were performed using Lipofectamine 3000 reagent (Invitrogen, Shandong, China) according to the manufacturer's instructions.

RNA extraction and quantitative real-time polymerase chain reaction (qRT-PCR)

Total RNA was extracted from cultured cells using RNA-easy Reagent (Vazyme, Jiangsu, China) and reverse-transcribed into cDNA using Hifair® III 1st Strand cDNA Synthesis SuperMix for qPCR (Yeasen, Shanghai, China) according to the manufacturer's protocols. qRT-PCR was performed using Hieff UNICON® qPCR SYBR Green Master Mix (Yeasen) to assess the expression levels of lncRNA, miRNA, and mRNA. Primers were provided by Tsingke (Beijing, China) and are listed in **Table 2**. Data were analyzed using the $2^{-\Delta\Delta Ct}$ method.

Cell proliferation assay

Cell proliferation was evaluated using an MTT assay kit (Meilunbio) according to the manufacturer's protocol. Cells were seeded into 96-well plates and incubated for 24, 48, 72, or 96 h. Absorbance was measured at 570 nm using a microplate reader.

Wound healing assay

After transfection, cell monolayers in 6-well plates were scratched uniformly using a 10 μL pipette tip and then incubated in serum-free medium. Cell migration was assessed by measuring the wound closure distance at 0 and 48 h after scratching.

Cell invasion assay

Cell invasion ability was evaluated using Matrigel-coated Transwell chambers. Matrigel (Corning, NY, USA) was thawed on ice and diluted 1:8 with pre-chilled serum-free medium. Then, 100 μL of the diluted Matrigel was evenly applied to the upper surface of the Transwell membrane and incubated at 37°C for 2 h to allow solidification. HCT-15 and HCT-116 cells from each treatment group were trypsinized, collected, counted, and resuspended in serum-free medium. A total of 2×10^5 cells in 200 μL of serum-free medium were seeded into the upper

Table 2. Primers of qRT-PCR

Target	Primer sequences (5'-3')
EWSAT1	Forward 5'-GTGTCTGGCAAGGAACACTA-3'
	Reverse 5'-GGTGGAGAAGAGGGACAATAAG-3'
miR-330-5p	Stem-loop 5'-GTCGTATCCAGTGCAGGGTCCGAGGTATTCGCACTGGATACGACTCTCTG-3'
	Forward 5'-GCAAAGCACACGGCCTG-3'
	Reverse 5'-GTGCAGGGTCCGAGGT-3'
CPEB4	Forward 5'-TGGGGATCAGCCTCTTCATA-3'
	Reverse 5'-CAATCCGCCTACAAACACCT-3'
β-actin	Forward 5'-TTGGTATCGTGGAAGGACTCA-3'
	Reverse 5'-TGTCATCATATTTGGCAGGTT-3'
U6	Forward 5'-GCTTCGGCAGCACATATACTAAAAT-3'
	Reverse 5'-CGCTTCACGAATTTGCGTGTCAT-3'

chamber. The lower chamber was filled with 500 μL of complete medium containing 10% fetal bovine serum as a chemoattractant. After incubation at 37°C in a 5% CO_2 incubator for 48 h, cells that had invaded through the Matrigel and attached to the lower surface of the membrane were fixed with 4% paraformaldehyde (Beyotime, China) for 30 min and stained with 0.1% crystal violet (Solarbio, China) for 30 min. After gentle washing with PBS and air drying, stained cells were observed and photographed under an optical microscope. Multiple random fields per chamber were counted to quantify invasive ability. All experiments were independently repeated three times.

Flow cytometry

After treatment, cells were collected, washed with PBS, and stained with Annexin V-fluorescein isothiocyanate (FITC, Meilunbio) and propidium iodide (PI) according to the manufacturer's protocol. Staining was performed for 15-20 min at room temperature in the dark. Apoptosis was analyzed using flow cytometry, and data were processed with FlowJo software.

Dual-luciferase reporter assay

Reporter plasmids carrying either wild-type (EWSAT1-wt, CPEB4-wt) or mutant (EWSAT1-mut, CPEB4-mut) miR-330-5p binding sites were obtained from Hunan Fenghui Biotechnology (Hunan, China). HEK293T cells were seeded into 96-well plates at 5×10^4 cells per well. When cells reached 60-70% confluence, co-transfections were performed using Lipofectamine 3000 reagent. Each co-transfection included one of the above reporter plasmids together with either miR-330-5p mimics or mimic control. After 48 h, firefly and Renilla luciferase activities were measured using a Luciferase Reporter Assay Kit (Meilunbio). Firefly luciferase signals were normalized to Renilla luciferase activity, which served as an internal control.

RNA pulldown assay

Biotin was ligated to the 3' ends of EWSAT1 and miR-330-5p. HCT-116 or HCT-15 cells were resuspended in lysis buffer containing 100 mM KCl, 5 mM $MgCl_2$, 20 mM Tris (pH 7.5), 0.3% NP-40, a protease inhibitor mixture (Roche, USA), and 50 U RNase OUT (Invitrogen, USA). CRC cell lysates were incubated with biotin-labeled EWSAT1 and miR-330-5p probes. The levels of lncRNA and miRNA were pulled down by biotin-labeled EWSAT1 and miR-330-5p pulldowns were detected by qRT-PCR.

Western blot

HCT-15 and HCT-116 cells from each treatment group were collected, washed with PBS, and lysed in RIPA buffer supplemented with a protease inhibitor mixture. Lysates were incubated on ice for 30 min, and the supernatant was collected as total protein extract. Protein concentration was determined using a BCA protein quantification kit. Equal amounts of protein from each group were separated by SDS-PAGE and transferred onto PVDF membranes. Membranes were blocked with 5% skim milk at room temperature for 1 h, followed by overnight incubation at 4°C with primary antibodies: anti-CPEB4 (1:1000; Proteintech, Wuhan, China) and anti-β-actin (1:2000; Proteintech, Wuhan,

China). After washing with TBST, membranes were incubated with HRP-conjugated secondary antibodies (goat anti-rabbit or goat anti-mouse IgG, 1:4000; Proteintech) for 1 h at room temperature. Protein bands were visualized using an ECL chemiluminescence reagent and quantified using ImageJ software. CPEB4 expression levels were normalized to β-actin.

Statistical methods

Continuous variables are presented as mean ± standard deviation (SD). All statistical analyses were performed using GraphPad Prism version 9.0. For clinical tissue analyses, differences in EWSAT1, miR-330-5p, and CPEB4 expression between paired CRC and adjacent normal tissues were assessed using paired Student's t-test. Correlations between gene expression levels in CRC tissues were evaluated using Pearson correlation analysis. Survival curves were generated using the Kaplan-Meier method, and differences between high- and low-expression groups were compared using the log-rank test. For in vitro experiments, all assays were independently repeated three times. Comparisons between two groups were performed using Student's t-test, whereas comparisons among multiple groups were analyzed using one-way ANOVA followed by Tukey's post hoc test. Cell proliferation curves from MTT assays were analyzed using two-way ANOVA followed by Tukey's multiple comparisons test. Dual-luciferase reporter assay data (wild-type vs. mutant) were also analyzed using two-way ANOVA.

Results

EWSAT1 was highly expressed in CRC and regulated malignant behavior

We first examined EWSAT1 expression in CRC patients. qRT-PCR was used to analyze EWSAT1 transcript levels in cancerous and adjacent normal tissues from 30 CRC patients. The results showed that EWSAT1 expression was significantly upregulated in CRC tissues compared with adjacent normal tissues (**Figure 1A**). Subsequently, we successfully knocked down EWSAT1 expression in CRC cell lines (HCT-15 and HCT-116) (**Figure 1B**) to investigate its effect on the malignant phenotype of CRC cells. MTT assays showed that EWSAT1 knockdown significantly inhibited CRC cell proliferation at 24, 48, 72, and 96 h (**Figure 1C**). Wound healing assays demonstrated that the migration rate of HCT-15 and HCT-116 cells transfected with si-EWSAT1 was significantly decreased compared with the control and nc groups (**Figure 1D**). Transwell invasion assays further confirmed that EWSAT1 knockdown significantly reduced the number of invasive HCT-15 and HCT-116 cells (**Figure 1E**). Furthermore, flow cytometry analysis showed that EWSAT1 knockdown significantly increased the apoptosis rate in both CRC cell lines (**Figure 1F**). These results indicated that high EWSAT1 expression is essential for proliferation, migration, and invasion of CRC cells while suppressing apoptosis.

EWSAT1 negatively regulated miR-330-5p expression in CRC

To further explore the downstream signaling pathways of EWSAT1, we used the starBase database to predict downstream miRNAs. Predicted binding sites between EWSAT1-wt and miR-330-5p are shown in **Figure 2A**. We also designed an EWSAT1-mut plasmid to mutate and inactivate the predicted binding sites. To clarify the expression pattern of miR-330-5p in CRC, we first validated its expression in the collected clinical samples. The results showed that miR-330-5p expression was significantly lower in CRC tissues than in adjacent normal tissues (**Figure 2B**) and was significantly negatively correlated with EWSAT1 expression (**Figure 2C**, $r=0.632$, $P < 0.0001$). To further clarify the regulatory relationship between the two, we performed an RNA pull-down assay and confirmed the pull-down efficiency of the biotin-labeled EWSAT1 probe by RT-qPCR (**Figure 2D**). The results showed that the EWSAT1 probe significantly enriched miR-330-5p in both CRC cell lines (**Figure 2E**). Furthermore, dual-luciferase reporter assays indicated that, after co-transfection of HEK293T cells with miR-330-5p mimics, the relative luciferase activity in the EWSAT1-wt group was significantly lower than in the EWSAT1-mut group (**Figure 2F**). This suggested that EWSAT1 specifically bound to miR-330-5p, consistent with the predicted results. In addition, knockdown of EWSAT1 upregulated miR-330-5p expression in CRC cells (**Figure 2G**). Furthermore, when EWSAT1-

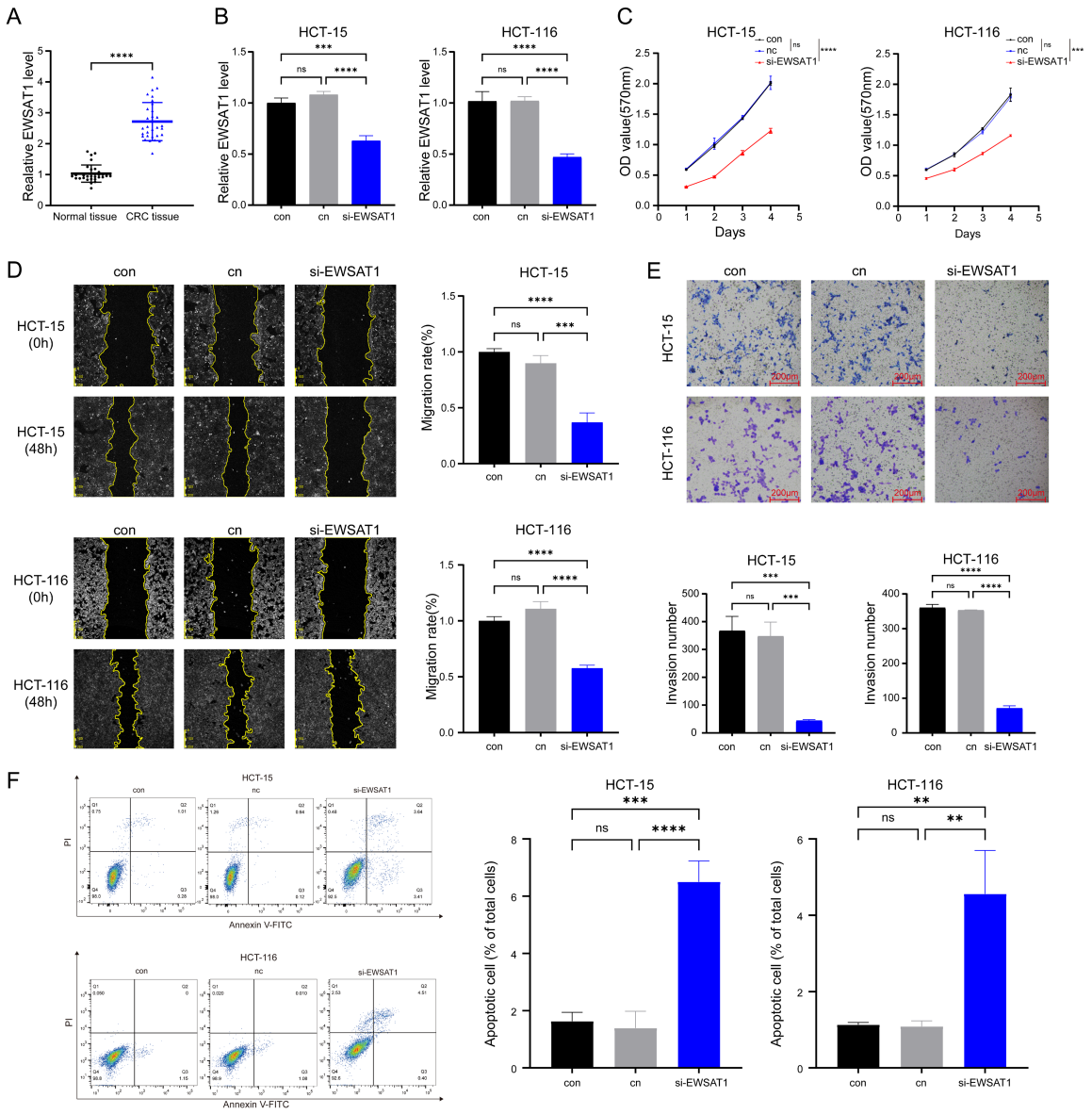

Figure 1. High expression of EWSAT1 in CRC tissues and its modulating malignant behavior. A: qRT-PCR detection of relative EWSAT1 expression in 30 paired CRC and adjacent normal tissues. B: qRT-PCR verification of knockdown efficiency after si-EWSAT1 transfection in HCT-15 and HCT-116 cells. C: MTT assay showing proliferation of HCT-15 and HCT-116 cells at different time points after EWSAT1 knockdown; OD values were measured at 570 nm. D: Wound healing assay showing the effect of EWSAT1 knockdown on migration of HCT-15 and HCT-116 cells at 0 and 48 h. Scale bar, 200 μm; original magnification, ×100. E: Transwell invasion assay showing the effect of EWSAT1 knockdown on invasion of HCT-15 and HCT-116 cells. Scale bar, 200 μm; original magnification, ×200. F: Annexin V-FITC/PI flow cytometry showing the effect of EWSAT1 knockdown on apoptosis of HCT-15 and HCT-116 cells. Data were presented as mean ± SD. Tissue samples were compared using a paired two-tailed Student's t-test. All cell experiments were performed in triplicate; comparisons among groups were performed using one-way ANOVA with Tukey's post hoc test. MTT proliferation curves were analyzed using two-way ANOVA. con, blank control group; nc, negative control group; si-EWSAT1, EWSAT1 knockdown group. ns, not significant; **P < 0.01; ***P < 0.001; ****P < 0.0001. EWSAT1, Ewing sarcoma-associated transcript 1; CRC, colorectal cancer; con, blank control group; nc, negative control group; si-EWSAT1, small interfering RNA targeting EWSAT1; FITC, fluorescein isothiocyanate; PI, propidium iodide.

knockdown cells were co-transfected with miR-330-5p antagomir, the upregulation of miR-330-5p induced by EWSAT1 knockdown was partially reversed (**Figure 2H**).

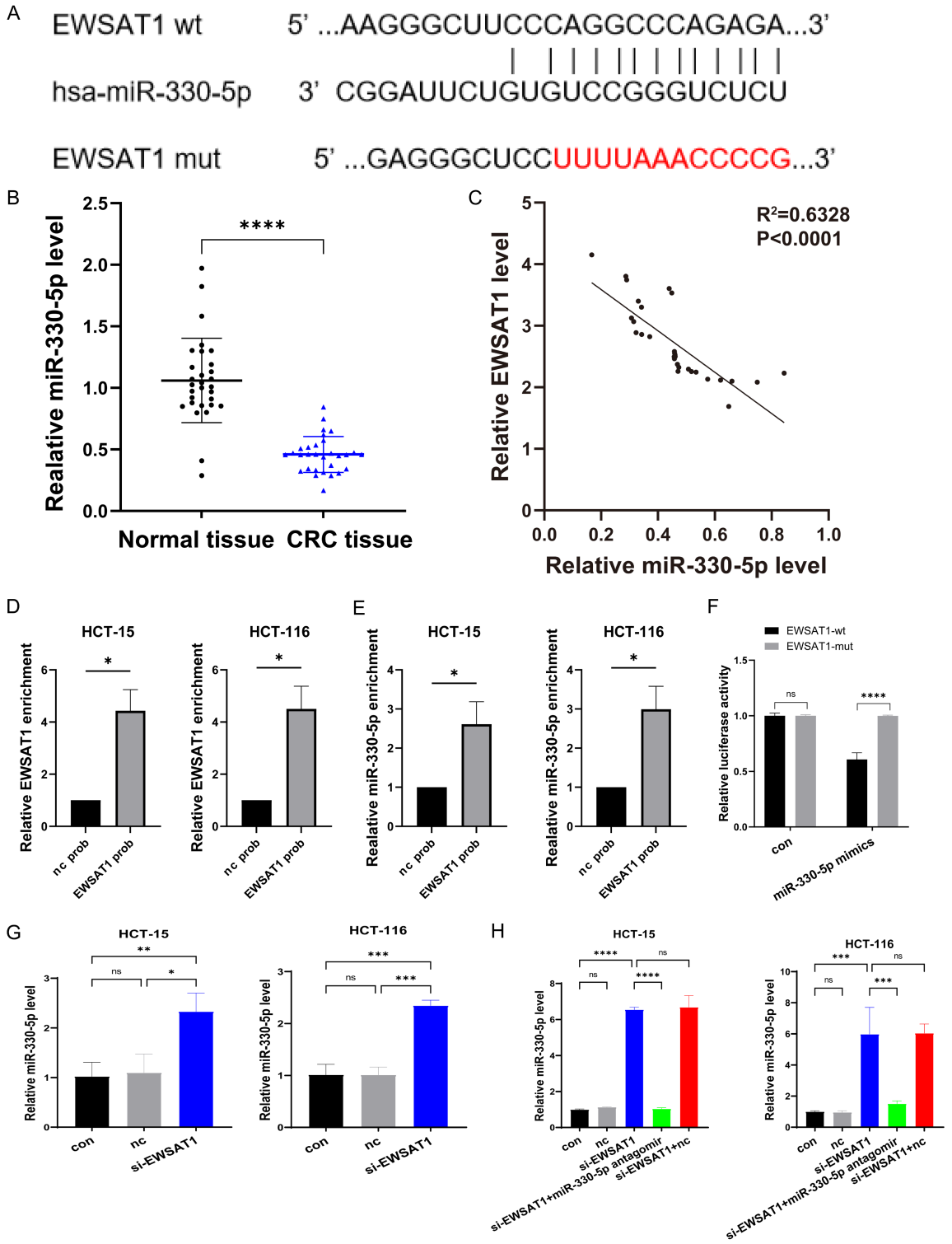

Figure 2. EWSAT1 bound to miR-330-5p and regulated its expression. A: StarBase prediction of potential binding sites between EWSAT1 and miR-330-5p, showing wild-type and mutant sequences of EWSAT1. B: qRT-PCR detection of relative miR-330-5p expression in 30 paired CRC and adjacent normal tissues. C: Pearson correlation analysis of the correlation between EWSAT1 and miR-330-5p expression levels in CRC tissues. D: Enrichment efficiency of the biotin-labeled EWSAT1 probe for EWSAT1 was detected after RNA pull-down. E: RNA pull-down assay showing enrichment of miR-330-5p by the EWSAT1 probe. F: Dual-luciferase reporter assay showing the effect of miR-330-5p mimics on the relative luciferase activity of EWSAT1-wt or EWSAT1-mut reporter vectors. G: qRT-PCR detection of

changes in miR-330-5p expression in HCT-15 and HCT-116 cells after EWSAT1 knockdown. H: qRT-PCR detection of the effect of miR-330-5p antagomir on EWSAT1 knockdown-induced changes in miR-330-5p expression. Data were presented as mean ± SD. Thirty paired clinical tissue samples were used; all cell experiments were performed in triplicate. Paired two-tailed Student's t-test was used for tissue comparisons. Pearson correlation analysis was used for correlation analysis. Two-tailed Student's t-test was used for cell experiment comparisons. Comparisons among multiple groups were performed using one-way ANOVA with Tukey's post hoc test. Dual-luciferase reporter assays were analyzed using two-way ANOVA followed by post hoc test. con, blank control group; nc, negative control group; wt, wild type; mut, mutant type; ns, not significant; $^{*}P < 0.05$; $^{**}P < 0.01$; $^{***}P < 0.001$; $^{****}P < 0.0001$. EWSAT1, Ewing sarcoma-associated transcript 1; hsa, Homo sapiens; miR, microRNA; CRC, colorectal cancer; wt, wild type; mut, mutant type; con, blank control group; nc, negative control group; probe, biotin-labeled probe; si-EWSAT1, small interfering RNA targeting EWSAT1.

EWSAT1 regulated the malignant behavior of CRC cells through miR-330-5p

To verify that EWSAT1 and miR-330-5p interact to regulate the malignant behavior of CRC, we co-transfected si-EWSAT1 and miR-330-5p antagomir into HCT-15 and HCT-116 cells. Compared with the control and nc groups, si-EWSAT1 transfection inhibited proliferation, migration, and invasion of CRC cells and increased the apoptosis rate. Co-transfection with si-EWSAT1 and miR-330-5p antagomir attenuated the si-EWSAT1-induced suppression of proliferation, migration, and invasion and also weakened the si-EWSAT1-promoted apoptosis of CRC cells (**Figure 3A-D**). These results suggest that EWSAT1 acts as a molecular sponge for miR-330-5p, thereby relieving miR-330-5p-mediated inhibition of its downstream target genes and affecting the malignant behavior of CRC cells.

miR-330-5p directly targeted and regulated expression of the downstream gene CPEB4

To elucidate the downstream target of miR-330-5p, we used the TargetScan bioinformatics prediction tool. The results showed potential binding sites between CPEB4-wt and miR-330-5p (**Figure 4A**). To confirm this regulatory relationship, we performed dual-luciferase assays. After co-transfection with miR-330-5p mimics, the relative luciferase activity of the CPEB4-wt group was significantly lower than that of the CPEB4-mut group, demonstrating that miR-330-5p directly bound to CPEB4 mRNA through complementary base pairing with its 3'UTR (**Figure 4B**). We next verified this regulatory relationship in clinical samples. qRT-PCR results showed that CPEB4 transcript levels were significantly higher in CRC tissues than in adjacent normal tissues (**Figure 4C**) and were negatively correlated with miR-330-5p expression (**Figure 4D**, r=0.69, P < 0.0001). At the cellular level, overexpression of miR-330-5p (**Figure 4E**) downregulated CPEB4 expression at both the mRNA and protein levels (**Figure 4F**, **4G**). These results indicated that CPEB4 is a direct functional target of miR-330-5p in CRC.

CPEB4 mediated the regulatory effects of EWSAT1 on malignant behaviors in CRC

To further clarify whether CPEB4 acts as a downstream effector of EWSAT1 in CRC progression, we first analyzed the correlation between their expression levels in the 30 paired CRC tissue samples. The results showed a significant positive correlation between EWSAT1 and CPEB4 expression (**Figure 5A**, r=0.557, P < 0.0001). Survival analysis based on follow-up data from these 30 patients revealed that patients with high CPEB4 expression had worse overall survival (**Figure 5B**, P=0.005). Consistent with this, Kaplan-Meier analysis using the public database GSE17536 also showed that high CPEB4 expression was associated with lower survival probability in CRC patients (**Figure 5C**, P=0.0015). Furthermore, at the cellular level, EWSAT1 knockdown significantly reduced CPEB4 expression in both HCT-15 and HCT-116 cells (**Figure 5D**).

To verify whether CPEB4 is involved in EWSAT1-mediated regulation of the CRC malignant phenotype, we performed a CPEB4 overexpression rescue experiment in EWSAT1-knockdown cells. qRT-PCR results confirmed that CPEB4 overexpression partially reversed the downregulation of CPEB4 induced by si-EWSAT1 (**Figure 5E**). Functional experiments showed that EWSAT1 knockdown significantly inhibited CRC cell proliferation, whereas CPEB4 overexpression partially reversed this inhibition (**Figure 5F**). Wound healing assays further demonstrated that CPEB4 overexpression restored the cell migration ability weakened by EWSAT1 knockdown (**Figure 5G**). Invasion assays showed that the decreased cell invasion ability induced

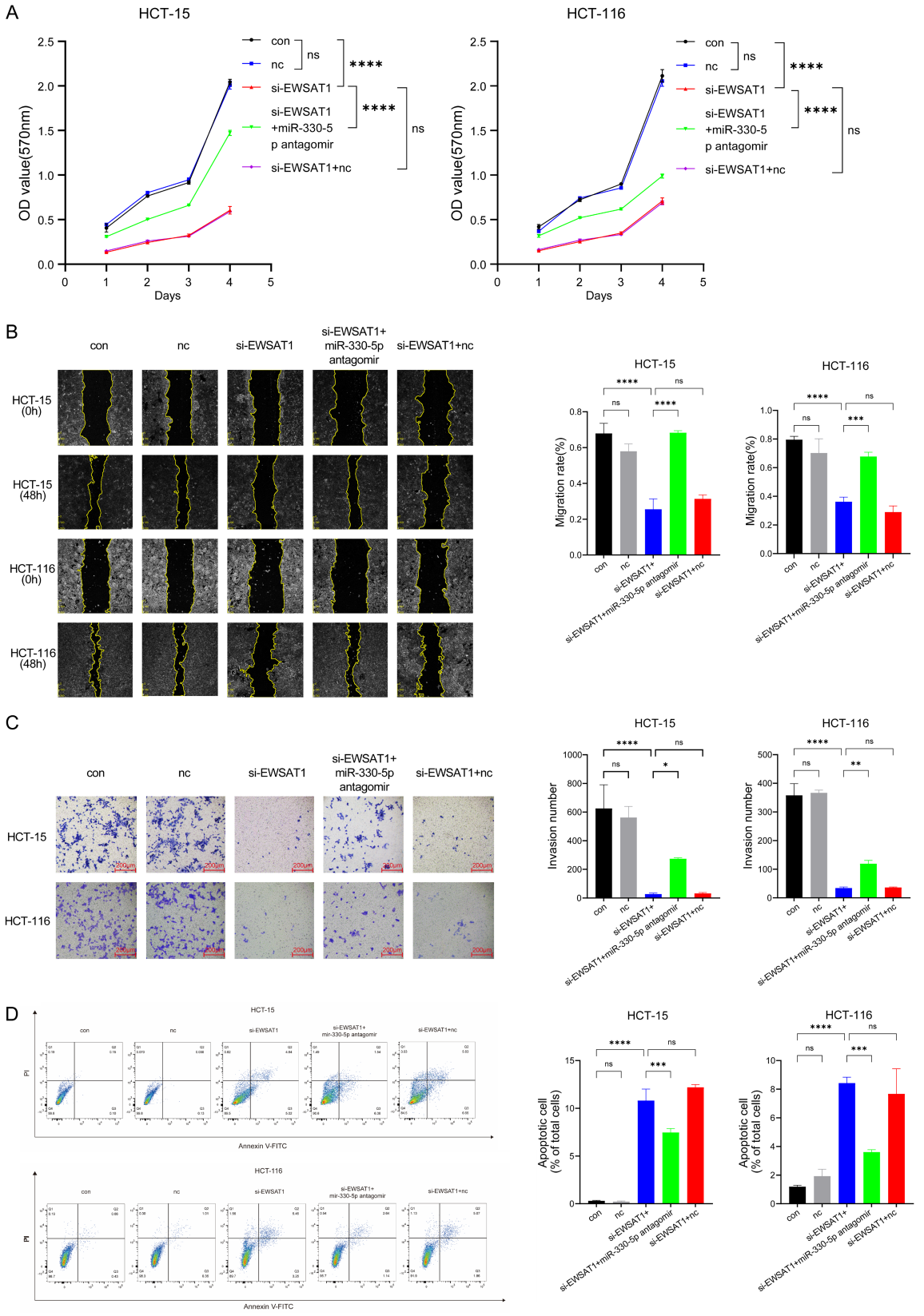

Figure 3. EWSAT1 regulated the malignant phenotype of CRC cells via miR-330-5p. A: MTT assay showing proliferation of HCT-15 and HCT-116 cells under different treatment conditions. B: Wound healing assay showing migration

of HCT-15 and HCT-116 cells at 0 and 48 h, together with quantitative analysis of migration rate. Scale bar, 200 μm; original magnification, ×100. C: Transwell invasion assay showing invasion of HCT-15 and HCT-116 cells after different treatments, together with quantification of invasive cell numbers. Scale bar, 200 μm; original magnification, ×200. D: Annexin V-FITC/PI flow cytometry showing apoptosis levels of CRC cells after different treatments, together with quantification of apoptotic cells. Data were presented as mean ± SD. All cell experiments were performed in triplicate. MTT proliferation curves were analyzed using two-way ANOVA with Tukey's multiple comparisons test. Other comparisons were performed using one-way ANOVA with Tukey's post hoc test. con, blank control group; nc, negative control group; si-EWSAT1, EWSAT1 knockdown group; miR-330-5p antagomir, miR-330-5p inhibitor. ns, not significant; $^{*}P < 0.05$; $^{**}P < 0.01$; $^{****}P < 0.0001$.

by si-EWSAT1 was also partially reversed by CPEB4 overexpression (**Figure 5H**). In addition, flow cytometry results showed that EWSAT1 knockdown significantly increased the proportion of apoptotic CRC cells, whereas CPEB4 overexpression attenuated this pro-apoptotic effect (**Figure 5I**).

Discussion

The diagnosis of CRC remains challenging, especially at early stages, leading to delayed detection and advanced-stage disease at presentation. Consequently, resectability rates are lower and mortality is higher [1, 2, 4, 5, 22]. Furthermore, although surgery, radiotherapy, chemotherapy, targeted therapy, and immunotherapy have significantly improved survival in some patients, recurrence, metastasis, and treatment failure remain major obstacles in CRC management, particularly for patients with advanced CRC [23]. Precision treatment of CRC is still limited by inadequate patient stratification [24, 25]. Currently, markers such as RAS, BRAF, MSI/MMR, and HER2 are commonly used in clinical practice to guide treatment [26]; however, these indicators primarily guide certain targeted therapy or immunotherapy decisions and do not fully explain the significant differences in proliferative capacity, invasion and metastasis, chemotherapy response, or prognosis among CRC patients [27, 28]. To address these unmet clinical needs, our study revealed a novel ceRNA regulatory network involved in the malignant progression of CRC. Our results showed that knockdown of EWSAT1 significantly inhibited proliferation, migration, and invasion of CRC cells while promoting apoptosis. This implies that EWSAT1 is not simply an aberrantly expressed molecule but rather an important functional lncRNA involved in maintaining the malignant phenotype of CRC.

LncRNAs have been shown to participate in tumorigenesis through multiple mechanisms, including chromatin remodeling, epigenetic regulation, transcriptional regulation, and post-transcriptional regulation of mRNA stability and translation [7, 29]. Among these, the ceRNA mechanism is a key pathway through which lncRNAs exert their pro- or anti-tumor effects. Specifically, lncRNAs can indirectly regulate the expression of protein-coding genes by competitively binding to specific miRNAs, thereby relieving miRNA-mediated suppression of downstream target mRNAs [8]. In CRC, several lncRNA-mediated ceRNA regulatory axes have been implicated in tumor progression. For example, ITGB8-AS1 acts as a ceRNA by binding to miR-33b-5p and let-7c/d-5p, thereby upregulating ITGA3/ITGB3 and activating the focal adhesion signaling pathway [9]; SNHG16 promotes CRC metastasis through the miR-124-3p/MCP-1 axis [10]; and miR600HG accelerates CRC progression via the miR-114-3p/KIF3A axis [11]. In addition, PCGEM1 exerts pro-tumor effects through the miR-433-3p/CTCF axis [30].

Therefore, we focused on EWSAT1 for further investigation. EWSAT1 was initially reported to be associated with Ewing's sarcoma [31], and has been shown to closely influence the malignant behavior of various tumors as a key regulator of ceRNA networks in osteosarcoma [32], cervical cancer [33] and glioma [34]. A meta-analysis by Wen et al. indicated that high EWSAT1 expression in various tumors predicted poor overall survival and was associated with adverse clinicopathological features [31]. However, EWSAT1 remains poorly studied in CRC, with only the study by Zhang et al. reporting that high EWSAT1 expression in CRC is closely related to proliferation and epithelial-mesenchymal transition, suggesting that high EWSAT1 expression may correlate with a highly invasive CRC phenotype [13]. Importantly, that study did not further explore the regulatory role of EWSAT1 in CRC. Our study systematically confirmed that EWSAT1 directly binds to miR-330-5p through bioinformatics prediction, expression correlation analysis, RNA pull-down,

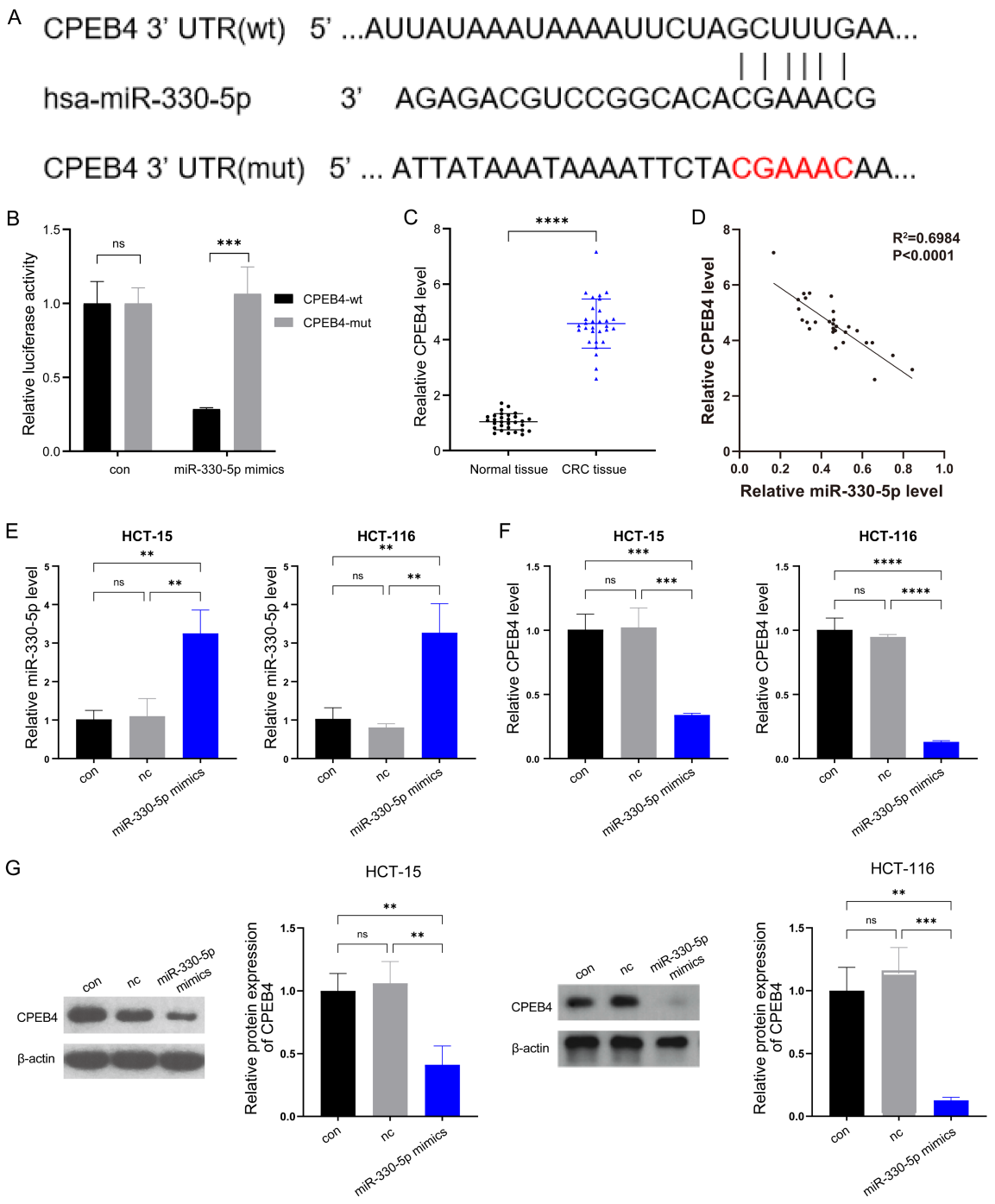

Figure 4. miR-330-5p directly targeted CPEB4 and inhibited its expression. A: TargetScan prediction of potential binding sites between miR-330-5p and the CPEB4 3'UTR, showing wild-type and mutant sequences of the CPEB4 3'UTR. B: Dual-luciferase reporter assay showing the effect of miR-330-5p mimics on the relative luciferase activity of CPEB4-wt or CPEB4-mut reporter vectors. C: qRT-PCR detection of relative CPEB4 expression in 30 paired CRC and adjacent normal tissues. D: Pearson correlation analysis of the correlation between miR-330-5p and CPEB4 expression levels in CRC tissues. E: qRT-PCR verification of transfection efficiency of miR-330-5p mimics in HCT-15 and HCT-116 cells. F: qRT-PCR detection of changes in CPEB4 mRNA expression in HCT-15 and HCT-116 cells after miR-330-5p overexpression. G: Western blot detection of changes in CPEB4 protein expression in HCT-15 and HCT-116 cells after miR-330-5p overexpression, with densitometric quantification using β-actin as an internal control. Data were presented as mean ± SD. Thirty paired clinical tissue samples were used; all cell experiments were performed in triplicate. Paired two-tailed Student's t-test was used for tissue comparisons. Pearson correlation analysis was used for correlation analysis. Comparisons among multiple groups were performed using one-way ANOVA with

Tukey's post hoc test. Dual-luciferase reporter assays were analyzed using two-way ANOVA followed by post hoc test. con, blank control group; nc, negative control group; wt, wild type; mut, mutant type. ns, not significant; $^{**}P < 0.01$; $^{***}P < 0.001$; $^{****}P < 0.0001$.

and dual-luciferase reporter assays. Furthermore, EWSAT1 and miR-330-5p showed opposite expression trends in CRC tissues and cells, suggesting that EWSAT1 may weaken the antitumor function of miR-330-5p through a molecular sponge effect.

MiRNAs play a critical role in carcinogenesis, and miR-330-5p is notably downregulated in CRC [35]. Consistent with this report, our results showed that overexpression of miR-330-5p significantly inhibited CRC cell proliferation, migration, and invasion and promoted apoptosis; conversely, inhibition of miR-330-5p reversed the suppression of malignant phenotypes induced by EWSAT1 knockdown. It is noteworthy that the biological role of miR-330-5p is not limited to CRC. Previous studies have shown that miR-330-5p is also involved in the development of various tumors, including breast cancer, bladder, and cervical cancers [16-18], suggesting a potentially universal tumor suppressor function. This evidence further underscores the potential therapeutic relevance of the EWSAT1/miR-330-5p regulatory axis in malignant tumors.

Notably, our study also identified CPEB4 as a direct target of miR-330-5p. Members of the CPEB family have been identified as cancer regulators [20]; CPEB4 binds to the cytoplasmic polyadenylation element (CPE) of target mRNAs and regulates cytoplasmic polyadenylation and translational activation during development [36, 37]. In tumors, CPEB4 has been reported to regulate ferroptosis in hepatocellular carcinoma [38], and its downregulation prevents non-small cell lung cancer invasion by inhibiting the ROS/Akt pathway [39]. In addition, CPEB4 promotes breast cancer metastasis by upregulating vimentin [40]. In CRC, CPEB4 remains relatively understudied. Early studies by Chi-Shuan Huang, Yu-Tien Chang, and colleagues analyzed gene expression profiles of peripheral blood samples from CRC patients and concluded that differential CPEB4 expression could be used for early CRC detection [41-43]. Notably, the study by Chi-Shuan Huang et al. further pointed out that CPEB4 may be involved not only in the translational regulation of mitosis in CRC but also in DNA replication [43]. In addition, a study by Xiaosheng He et al. indicated that CPEB4 has prognostic value in CRC, with high CPEB4 expression associated with worse prognosis, which is consistent with our clinical data [44]. Furthermore, a study by Annarita Sibilio et al. on precancerous lesions of CRC emphasized that CPEB4 maintains intestinal homeostasis; chronic CPEB4 overexpression causes dysregulation of IL-22 expression, which promotes the transformation of inflammatory bowel disease to CRC [45].

Based on the above findings, this study has the following potential clinical implications. First, exosomal miRNAs are promising tools for diagnostics and therapeutics. Exosomes, approximately 100-nm lipid-bilayer vesicles that are abundant in biofluids [46, 47], carry functional miRNAs that control tumor proliferation, angiogenesis, and metastasis [48, 49]. For example, exosomal miR-144-3p inhibits osteosarcoma progression [50]. Given the tumor-suppressive function of miR-330-5p, its presence in exosomes could serve two purposes: (1) as an alternative liquid biopsy marker for early CRC detection, complementing current markers such as CEA and improving diagnostic specificity; and (2) as a therapeutic carrier, where miR-330-5p can be packaged into exosomes to achieve targeted delivery to the tumor site while reducing systemic toxicity [51]. In conclusion, our study illuminates how the EWSAT1/miR-330-5p/CPEB4 axis controls CRC development. By validating the ceRNA activity of EWSAT1 on miR-330-5p and the subsequent de-repression of CPEB4, we offer mechanistic insights with direct clinical relevance for novel diagnostics and targeted therapy in CRC.

This study has several limitations. First, the clinical sample size is relatively small; expression validation, correlation analysis, and survival analysis were conducted using tissue samples from only 30 CRC patients. The limited sample size may reduce statistical power and limit the generalizability of the conclusions. The clinical significance of the EWSAT1/miR-330-5p/CPEB4 axis requires further validation in larger, multicenter cohorts across different tumor stages, molecular subtypes, and treat-

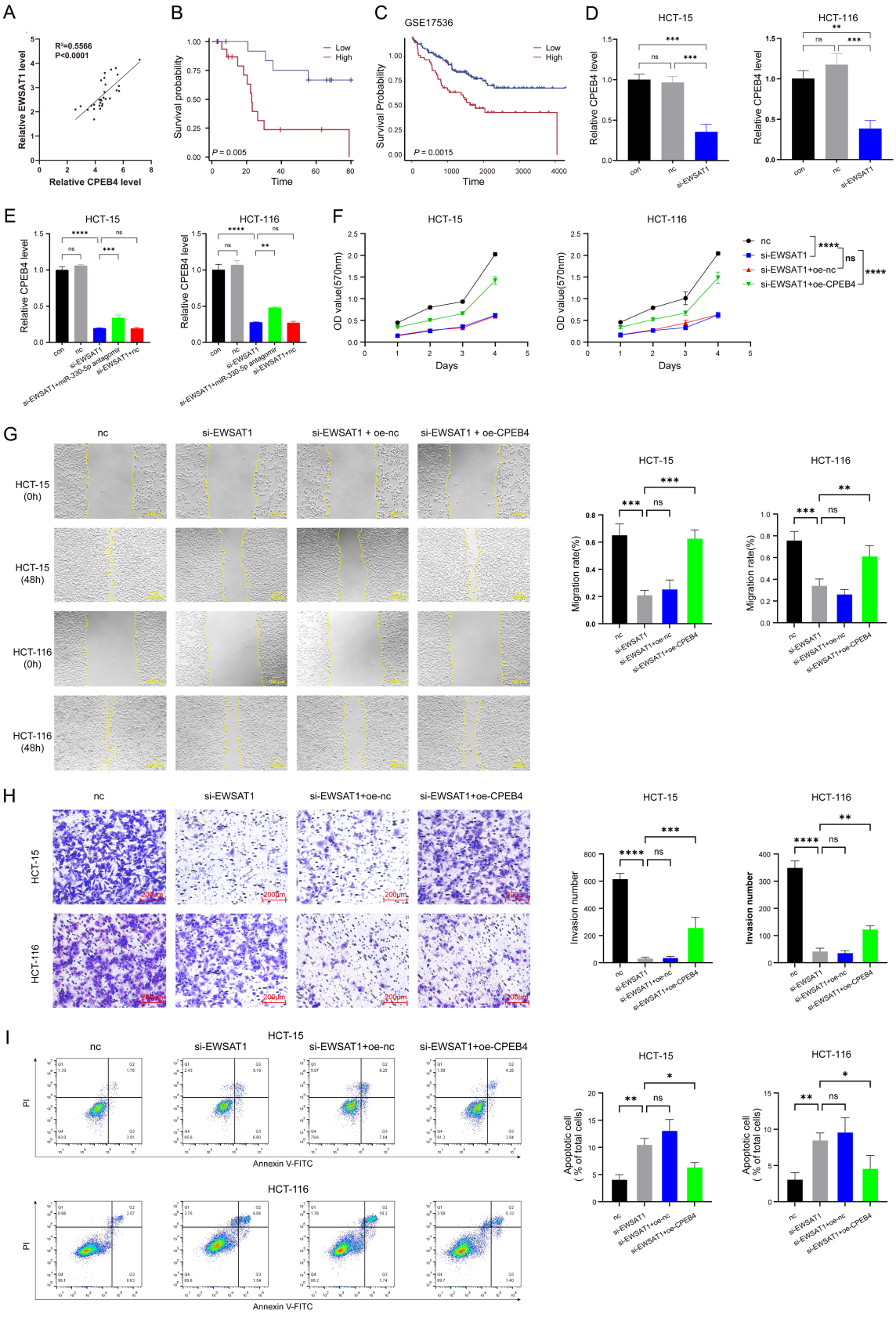
A
R²=0.5566
P<0.0001
Relative EWSAT1 level
Relative CPEB4 level
B
Survival probability
Low
High
P = 0.005
Time
C
GSE17536
Survival Probability
Low
High
P = 0.0015
Time
D
HCT-15
HCT-116
Relative CPEB4 level
con
nc
si-EWSAT1
E
HCT-15
HCT-116
Relative CPEB4 level
si-EWSAT1+miR-330-5p antagomir
si-EWSAT1+nc
F
HCT-15
HCT-116
OD value(570nm)
Days
nc
si-EWSAT1
si-EWSAT1+oe-nc
si-EWSAT1+oe-CPEB4
G
nc
si-EWSAT1
si-EWSAT1 + oe-nc
si-EWSAT1 + oe-CPEB4
HCT-15 (0h)
HCT-15 (48h)
HCT-116 (0h)
HCT-116 (48h)
Migration rate(%)
H
si-EWSAT1+oe-nc
si-EWSAT1+oe-CPEB4
Invasion number
I
Annexin V-FITC
PI
Apoptotic cell (% of total cells)

Figure 5. CPEB4 mediated EWSAT1-regulated malignant phenotypes in CRC cells. (A) Correlation between EWSAT1 and CPEB4 expression in 30 CRC tissue samples. (B) Kaplan-Meier survival analysis of CRC patients stratified by CPEB4 expression in the collected cohort. (C) Kaplan-Meier survival analysis of CPEB4 expression in the GSE17536 cohort. (D) CPEB4 expression in HCT-15 and HCT-116 cells after EWSAT1 knockdown. (E) qRT-PCR validation of CPEB4 overexpression in EWSAT1-knockdown cells. (F) MTT assays showing the effect of CPEB4 overexpression on cell proliferation after EWSAT1 knockdown. (G) Wound healing assay showing changes in cell migration at 0 and 48 h, together with quantitative analysis of migration rate. Scale bar, 200 μm; original magnification, ×100. (H) Transwell invasion assay showing changes in cell invasion, together with quantification of invasive cell numbers. Representative crystal violet-stained images are shown. Scale bar, 200 μm; original magnification, ×200. (I) Annexin V-FITC/PI flow cytometry showing changes in cell apoptosis, together with quantification of apoptotic cells. Data are presented as mean ± SD. Cell experiments were performed in triplicate. Pearson correlation analysis was used in (A). Survival curves were compared using the log-rank test. MTT curves were analyzed using two-way ANOVA followed by Tukey's multiple comparisons test. Other multi-group comparisons were analyzed using one-way ANOVA followed by Tukey's post hoc test. nc, negative control; si-EWSAT1, EWSAT1 knockdown; oe-nc, overexpression negative control; oe-CPEB4, CPEB4 overexpression. ns, not significant; $^{**}P < 0.01$; $^{***}P < 0.001$; $^{****}P < 0.0001$.

ment backgrounds. Second, this study relied primarily on two CRC cell lines, HCT-15 and HCT-116, for in vitro functional experiments. Although our results suggest that EWSAT1 knockdown inhibits proliferation, migration, and invasion and promotes apoptosis in CRC cells, cell models cannot fully recapitulate the in vivo tumor microenvironment, including immune regulation, angiogenesis, and metastasis. Therefore, the biological role of this molecular axis in CRC development and progression needs to be further confirmed using in vivo models such as subcutaneous tumorigenesis, orthotopic tumor models, or metastatic models. Third, although this study supported the role of EWSAT1 as a ceRNA regulating the miR-330-5p/CPEB4 axis through RNA pull-down, dual-luciferase reporter assays, and rescue experiments, we have not yet systematically evaluated the subcellular localization of EWSAT1, the molecular abundance relationship between EWSAT1 and miR-330-5p, or the downstream translational regulatory network of CPEB4. Future studies should combine RNA-FISH, AGO2-RIP, in vivo functional validation, and multi-omics analyses to further clarify the functional boundaries and clinical translational value of this axis in CRC progression, metastasis, and treatment response.

Acknowledgements

This work was supported by the Qingdao Medical and Health Research Guidance Project (Grant No. 2025-WJKY058).

Disclosure of conflict of interest

None.

Address correspondence to: Tao Yang, Department of General Surgery, Qingdao Central Hospital, University of Health and Rehabilitation Sciences, No. 127, Siliu South Road, Shibei District, Qingdao 266042, Shandong, China. E-mail: yangtao2025-08@163.com

References

[1] Bray F, Laversanne M, Sung H, Ferlay J, Siegel RL, Soerjomataram I and Jemal A. Global cancer statistics 2022: GLOBOCAN estimates of incidence and mortality worldwide for 36 cancers in 185 countries. CA Cancer J Clin 2024; 74: 229-263.

[2] Siegel RL, Wagle NS, Cercek A, Smith RA and Jemal A. Colorectal cancer statistics, 2023. CA Cancer J Clin 2023; 73: 233-254.

[3] Wu Y, Li Y, Wang X, Zhou X, Yan X, Wang H, Zhu J, Chen W and Shi J. Disability-adjusted life years for colorectal cancer in China, 2017-2030: a prevalence-based analysis focusing on the impact of screening coverage and the application of local weights. Chin Med J (Engl) 2025; 138: 962-972.

[4] Fritz CDL, Otegbeye EE, Zong X, Demb J, Nickel KB, Olsen MA, Mutch M, Davidson NO, Gupta S and Cao Y. Red-flag signs and symptoms for earlier diagnosis of early-onset colorectal cancer. J Natl Cancer Inst 2023; 115: 909-916.

[5] Eng C, Jácome AA, Agarwal R, Hayat MH, Byndloss MX, Holowatyj AN, Bailey C and Lieu CH. A comprehensive framework for early-onset colorectal cancer research. Lancet Oncol 2022; 23: e116-e128.

[6] Chodurska B and Kunej T. Long non-coding RNAs in humans: classification, genomic organization and function. Noncoding RNA Res 2025; 11: 313-327.

[7] Tan YT, Lin JF, Li T, Li JJ, Xu RH and Ju HQ. LncRNA-mediated posttranslational modifications and reprogramming of energy metabolism in cancer. Cancer Commun (Lond) 2021; 41: 109-120.

[8] Bhattacharjee R, Prabhakar N, Kumar L, Bhattacharjee A, Kar S, Malik S, Kumar D, Ruoko-

lainen J, Negi A, Jha NK and Kesari KK. Crosstalk between long noncoding RNA and microRNA in cancer. Cell Oncol (Dordr) 2023; 46: 885-908.
[9] Lin X, Zhuang S, Chen X, Du J, Zhong L, Ding J, Wang L, Yi J, Hu G, Tang G, Luo X, Liu W and Ye F. lncRNA ITGB8-AS1 functions as a ceRNA to promote colorectal cancer growth and migration through integrin-mediated focal adhesion signaling. Mol Ther 2022; 30: 688-702.
[10] Chen ZY, Wang XY, Yang YM, Wu MH, Yang L, Jiang DT, Cai H and Peng Y. LncRNA SNHG16 promotes colorectal cancer cell proliferation, migration, and epithelial-mesenchymal transition through miR-124-3p/MCP-1. Gene Ther 2022; 29: 193-205.
[11] Huang Y, Wang L and Liu D. lncRNA MIR600HG induces the proliferation and invasion of colorectal cancer cells via regulating miR-144-3p/KIF3A. Int Immunopharmacol 2022; 108: 108686.
[12] Aryee DNT, Fock V, Kapoor U, Radic-Sarikas B and Kovar H. Zooming in on long non-coding RNAs in Ewing sarcoma pathogenesis. Cells 2022; 11: 1267.
[13] Zhang R, Li JB, Yan XF, Jin K, Li WY, Xu J, Zhao J, Bai JH and Chen YZ. Increased EWSAT1 expression promotes cell proliferation, invasion and epithelial-mesenchymal transition in colorectal cancer. Eur Rev Med Pharmacol Sci 2018; 22: 6801-6808.
[14] Seida M, Ogami K, Yoshino S and Suzuki HI. Fine regulation of microRNAs in gene regulatory networks and pathophysiology. Int J Mol Sci 2025; 26: 2861.
[15] Nazki FH and Bracken CP. Regulation and dysregulation of microRNA - transcription factor axes in differentiation and neuroblastoma. Cell Mol Life Sci 2025; 82: 304.
[16] Wang MH, Liu ZH, Zhang HX, Liu HC and Ma LH. Hsa_circRNA_000166 accelerates breast cancer progression via the regulation of the miR-326/ELK1 and miR-330-5p/ELK1 axes. Ann Med 2024; 56: 2424515.
[17] Zhong J, Xu A, Xu P, Su M, Wang P, Liu Z, Li B, Liu C and Jiang N. Circ_0000235 targets MCT4 to promote glycolysis and progression of bladder cancer by sponging miR-330-5p. Cell Death Discov 2023; 9: 283.
[18] Hou S, Zhang X and Yang J. Long non-coding RNA ABHD11-AS1 facilitates the progression of cervical cancer by competitively binding to miR-330-5p and upregulating MARK2. Exp Cell Res 2022; 410: 112929.
[19] Lu C, Fu L, Qian X, Dou L and Cang S. Knockdown of circular RNA circ-FARSA restricts colorectal cancer cell growth through regulation of miR-330-5p/LASP1 axis. Arch Biochem Biophys 2020; 689: 108434.
[20] Li J, Wu Y, Zhang D, Zhang Z, Li S, Cheng X, Chen L, Zhou G and Yuan C. The roles of cytoplasmic polyadenylation element binding protein 1 in tumorigenesis. Mini Rev Med Chem 2024; 24: 2008-2018.
[21] Fernández-Alfara M, Sibilio A, Martin J, Tusquets Uxó E, Malumbres M, Alcalde V, Chanes V, Cañellas-Socias A, Palomo-Ponce S, Batlle E and Méndez R. Antitumor T-cell function requires CPEB4-mediated adaptation to chronic endoplasmic reticulum stress. EMBO J 2023; 42: e111494.
[22] Li N, Lu B, Luo C, Cai J, Lu M, Zhang Y, Chen H and Dai M. Incidence, mortality, survival, risk factor and screening of colorectal cancer: a comparison among China, Europe, and northern America. Cancer Lett 2021; 522: 255-268.
[23] Roshandel G, Ghasemi-Kebria F and Malekzadeh R. Colorectal cancer: epidemiology, risk factors, and prevention. Cancers (Basel) 2024; 16: 1530.
[24] Hu R, Qiu Y, Liu DA, Chen S, Chen K, Xu Y, Yuan J, Zhang X and Li X. Advances in intestinal flora for the development, diagnosis and treatment of CRC. Front Microbiol 2025; 16: 1495274.
[25] Hossain MS, Karuniawati H, Jairoun AA, Urbi Z, Ooi J, John A, Lim YC, Kibria KMK, Mohiuddin AKM, Ming LC, Goh KW and Hadi MA. Colorectal cancer: a review of carcinogenesis, global epidemiology, current challenges, risk factors, preventive and treatment strategies. Cancers (Basel) 2022; 14: 1732.
[26] Morris VK, Kennedy EB, Baxter NN, Benson AB 3rd, Cercek A, Cho M, Ciombor KK, Cremolini C, Davis A, Deming DA, Fakih MG, Gholami S, Hong TS, Jaiyesimi I, Klute K, Lieu C, Sanoff H, Strickler JH, White S, Willis JA and Eng C. Treatment of metastatic colorectal cancer: ASCO guideline. J Clin Oncol 2023; 41: 678-700.
[27] Dang Q, Zuo L, Hu X, Zhou Z, Chen S, Liu S, Ba Y, Zuo A, Xu H, Weng S, Zhang Y, Luo P, Cheng Q, Liu Z and Han X. Molecular subtypes of colorectal cancer in the era of precision oncotherapy: current inspirations and future challenges. Cancer Med 2024; 13: e70041.
[28] Sobral D, Martins M, Kaplan S, Golkaram M, Salmans M, Khan N, Vijayaraghavan R, Casimiro S, Fernandes A, Borralho P, Ferreira C, Pinto R, Abreu C, Costa AL, Zhang S, Pawlowski T, Godsey J, Mansinho A, Macedo D, Lobo-Martins S, Filipe P, Esteves R, Coutinho J, Costa PM, Ramires A, Aldeia F, Quintela A, So A, Liu L, Grosso AR and Costa L. Genetic and microenvironmental intra-tumor heterogeneity impacts colorectal cancer evolution and metastatic development. Commun Biol 2022; 5: 937.
[29] Bridges MC, Daulagala AC and Kourtidis A. LNCcation: lncRNA localization and function. J Cell Biol 2021; 220: e202009045.
[30] Xu W, Wu L, Lu H, Xiang X, Wang F and Li S. LncRNA PCGEM1 promotes colorectal cancer cell proliferation and migration in positive

feedback loop through PCGEM1/miR-433-3p/CTCF axis. Pathol Res Pract 2022; 237: 154017.
[31] Wen J, Li H, Li D and Dong X. Clinicopathological and prognostic significance of long noncoding RNA EWSAT1 in human cancers: a review and meta analysis. PLoS One 2022; 17: e0265264.
[32] Shen D, Liu Y, Liu Y, Wang T, Yuan L, Huang X and Wang Y. Long non-coding RNA EWSAT1 promoted metastasis and actin cytoskeleton changes via miR-24-3p sponging in osteosarcoma. J Cell Mol Med 2021; 25: 716-728.
[33] Zhou Q, Xie Y, Wang L, Xu T and Gao Y. LncRNA EWSAT1 upregulates CPEB4 via miR-330-5p to promote cervical cancer development. Mol Cell Biochem 2020; 471: 177-188.
[34] Yang H, Chen W, Jiang G, Yang J, Wang W and Li H. Long non-coding RNA EWSAT1 contributes to the proliferation and invasion of glioma by sponging miR-152-3p. Oncol Lett 2020; 20: 1846-1854.
[35] Liu J, Yue K, Yang J, Bi C, Zhang Y and Zhang W. miR-330-5p suppress cell growth and invasion via disrupting HSF4-mediated MACC1/STAT3 pathway in colorectal cancer. Front Biosci (Landmark Ed) 2024; 29: 53.
[36] Huang YS, Mendez R, Fernandez M and Richter JD. CPEB and translational control by cytoplasmic polyadenylation: impact on synaptic plasticity, learning, and memory. Mol Psychiatry 2023; 28: 2728-2736.
[37] Ji J, Xu Y, Wang Y, Zhang G, Tian X, Zhang Y and Ren J. miR-351-5p regulation of CPEB3 affecting aluminium-induced learning and memory impairment in SD rats. Environ Pollut 2024; 362: 124973.
[38] Delgado ME, Naranjo-Suarez S, Ramírez-Pedraza M, Cárdenas BI, Gallardo-Martínez C, Balvey A, Belloc E, Martín J, Boyle M, Méndez R and Fernandez M. CPEB4 modulates liver cancer progression by translationally regulating hepcidin expression and sensitivity to ferroptosis. JHEP Rep 2024; 7: 101296.
[39] Hu J, Zhang L, Chen Q, Lin J, Wang S, Liu R, Zhang W, Miao K and Shou T. Knockdown of CPEB4 expression suppresses cell migration and invasion via Akt pathway in non-small cell lung cancer. Cell Biol Int 2018; 42: 1484-1491.
[40] Lu R, Zhou Z, Yu W, Xia Y and Zhi X. CPEB4 promotes cell migration and invasion via upregulating Vimentin expression in breast cancer. Biochem Biophys Res Commun 2017; 489: 135-141.
[41] Chang YT, Yao CT, Su SL, Chou YC, Chu CM, Huang CS, Terng HJ, Chou HL, Wetter T, Chen KH, Chang CW, Shih YW and Lai CH. Verification of gene expression profiles for colorectal cancer using 12 internet public microarray datasets. World J Gastroenterol 2014; 20: 17476-17482.
[42] Chang YT, Huang CS, Yao CT, Su SL, Terng HJ, Chou HL, Chou YC, Chen KH, Shih YW, Lu CY, Lai CH, Jian CE, Lin CH, Chen CT, Wu YS, Lin KS, Wetter T, Chang CW and Chu CM. Gene expression profile of peripheral blood in colorectal cancer. World J Gastroenterol 2014; 20: 14463-14471.
[43] Huang CS, Terng HJ and Hwang YT. Gene-function-based clusters explore intricate networks of gene expression of circulating tumor cells in patients with colorectal cancer. Biomedicines 2023; 11: 145.
[44] He X, Lin X, Cai M, Fan D, Chen X, Wang L, Wu X, Lan P and Wang J. High expression of cytoplasmic polyadenylation element-binding protein 4 correlates with poor prognosis of patients with colorectal cancer. Virchows Arch 2017; 470: 37-45.
[45] Sibilio A, Suñer C, Fernández-Alfara M, Martín J, Berenguer A, Calon A, Chanes V, Millanes-Romero A, Fernández-Miranda G, Batlle E, Fernández M and Méndez R. Immune translational control by CPEB4 regulates intestinal inflammation resolution and colorectal cancer development. iScience 2022; 25: 103790.
[46] Liu J, Ren L, Li S, Li W, Zheng X, Yang Y, Fu W, Yi J, Wang J and Du G. The biology, function, and applications of exosomes in cancer. Acta Pharm Sin B 2021; 11: 2783-2797.
[47] Théry C, Zitvogel L and Amigorena S. Exosomes: composition, biogenesis and function. Nat Rev Immunol 2002; 2: 569-579.
[48] Conigliaro A, Costa V, Lo Dico A, Saieva L, Buccheri S, Dieli F, Manno M, Raccosta S, Mancone C, Tripodi M, De Leo G and Alessandro R. CD90+ liver cancer cells modulate endothelial cell phenotype through the release of exosomes containing H19 lncRNA. Mol Cancer 2015; 14: 155.
[49] Li B, Cao Y, Sun M and Feng H. Expression, regulation, and function of exosome-derived miRNAs in cancer progression and therapy. FASEB J 2021; 35: e21916.
[50] Jiang M, Jike Y, Liu K, Gan F, Zhang K, Xie M, Zhang J, Chen C, Zou X, Jiang X, Dai Y, Chen W, Qiu Y and Bo Z. Exosome-mediated miR-144-3p promotes ferroptosis to inhibit osteosarcoma proliferation, migration, and invasion through regulating ZEB1. Mol Cancer 2023; 22: 113.
[51] Liang Y, Duan L, Lu J and Xia J. Engineering exosomes for targeted drug delivery. Theranostics 2021; 11: 3183-3195.